ACS APPLIED MATERIALS & INTERFACES
Research Article
www.acsami.org

Diffusion Barrier and Adhesion Properties of SiO_xN_y and SiO_x Layers between Ag/Polypyrrole Composites and Si Substrates

Barbara Horváth,* Jin Kawakita, and Toyohiro Chikyow

MANA, National Institute for Materials Science (NIMS), 1-1 Namiki, Tsukuba, Ibaraki 305-0044, Japan

ABSTRACT: This paper describes the interface reactions and diffusion between silver/polypyrrole (Ag/PPy) composite and silicon substrate. This composite material can be used as a novel technique for 3D-LSI (large-scale integration) by the fast infilling of through-silicon vias (TSV). By immersion of the silicon wafer with via holes into the dispersed solution of Ag/PPy composite, the holes are filled with the composite. It is important to develop a layer between the composite and the Si substrate with good diffusion barrier and adhesion characteristics. In this paper, SiO_x and two types of SiO_xN_y barrier layers with various thicknesses were investigated. The interface structure between the Si substrate, the barrier, and the Ag/PPy composite was characterized by transmission electron microscopy. The adhesion and diffusion properties of the layers were established for Ag/PPy composite. Increasing thickness of SiO_x proved to permit less Ag to transport into the Si substrate. SiO_xN_y barrier layers showed very good diffusion barrier characteristics; however, their adhesion depended strongly on their composition. A barrier layer composition with good adhesion and Ag barrier properties has been identified in this paper. These results are useful for filling conductive metal/polymer composites into TSV.

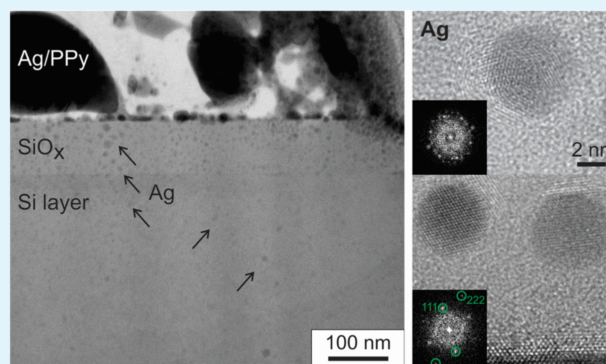

KEYWORDS: *flexible composites, barrier layers, oxides, diffusion, adhesion*

1. INTRODUCTION

As a direct consequence of Moore's law, downsizing of large-scale integration (LSI) for improved performance is expected to reach its limit in the near future with the continuous demand for higher packing density and lower power. For further integration of LSI, the chips are stacked vertically, known as 3D-LSI (large-scale integration). While there are many methods to connect the chips (such as wire-bonding), the latest and most effective method is by direct contact between the layers. The key technology for this is the through-silicon via (TSV) where conductive electrical wiring is provided in the vertical direction between the LSI chips in a via form.[1]

Currently, copper electroplating is the preferred method for filling conductive material into these vias,[2,3] although it takes more than 1 h to complete the process including the pretreatment.[4] Apart from the long creation time, Cu electroplating has several other bad properties as well, such as multiple processing steps throughout production, difficulty to create deep TSVs with high aspect ratios, large differences in coefficient of thermal expansion (CTE) between Si and Cu (CTE ~ 3 and 17 ppm/K, respectively),[5] and the rapid and aggressive diffusion of Cu into Si or SiO_2.[6]

We are developing composites of metal and conducting polymer to obtain a faster TSV infilling method by the immersion of a Si wafer obtained with vias into a dispersed solution of this composite. These composites are useful for TSV filling because it is a good replacement for Cu electroplating. Most conductive polymers have relatively low electrical conductivity properties; however, by forming composites with additional metals such as Ag,[7] Pd,[8] or Au,[9,10] good conductive performance can be achieved, making it applicable for electronic devices. The composites discussed in this paper are produced by the oxidation of pyrrole with Ag ions, with a photoassisted reaction occurring by UV irradiation, increasing the growth rate of the composite. The combination of silver with the conducting polypyrrole (PPy) resulted in highly conductive (2×10^4 $\Omega^{-1}\cdot cm^{-1}$) composite, which is hundreds of times higher than the commercial conducting polymers.[11] The structure of the dispersed conducting polymer-coated colloidal particles has been observed by various reports in the past. Depending on the reaction conditions, the structure can be varied from single Ag-core structure with the polypyrrole acting as a shell,[12−14] to a raspberry-like structure where Ag is located on the surface of a polymer.[12,15,16] Until now, the main uses of conducting Ag/PPy composites were for gas sensors,[17,18] catalysis,[19,20] antimicrobial coating,[21,22] or inkjet printed conducting wiring for flexible electronics.[7] Ag/PPy composite has been proved as an excellent material for the electric wiring of flexible electronic devices, as it is conductive, flexible, cheap and has sufficient adhesion to the substrate.

Received: March 4, 2014
Accepted: May 28, 2014
Published: May 28, 2014

ACS Publications © 2014 American Chemical Society

By the use of this composite as a filling material for TSVs, the via filling process may be shortened down to only 10 min.[23] Ag/PPy coatings have excellent adhesive properties toward several substrates, such as Si and various plastics (i.e, polytetrafluoroethylene, polyimide),[24] making the material also a reliable candidate as a TSV material. Reports have shown good adhesion properties of pure Py and PPy on Si,[25] and the liquid dispersite of Ag/PPy has very good wetting properties on Si and SiO_2 surfaces with average contact angles of 27.8° and 10.3°, respectively.[23] The low angle reflects high strength of the molecular interaction between the dispersion and the substrate, providing good adhesion between the two materials. Ag nanoparticles, however, may be possible diffusers toward the Si substrate. Although they may have a positive role on the adhesion, they can cause reliability issues and reduce the lifespan of electronic devices.[26−28]

The phenomenon of impurity diffusion can be prevented by the use of barrier layers, which prohibit the diffusion of the atoms into the substrate. SiO_x and SiN_x are widely used in Si chip manufacturing for TSV development. Currently, SiO_2 is primarily used as via liner to cover any defect the via etching may have caused and to electrically isolate the filling material from the substrate.[29,30] An obvious choice as barrier for the Ag/PPy material could be the use of SiO_x and SiN_x, but while SiN_x has good barrier properties to Ag diffusion,[31,32] its adhesion toward polymers is poor[33] and extra treatment steps (such as adhesion promoter) are necessary to improve this property, which puts an additional step in the throughput of the via. SiO_x is found to have poor diffusion barrier properties when examined with Ag pastes.[34] SiO_xN_y, which may contain some properties of SiN_x and SiO_x, however, yet has not been evaluated thoroughly. While there is limited research on its Ag diffusion barrier properties,[35] there are no precise specifics of the composition.

An aim of this paper, therefore, is to find a suitable barrier layer that shows good adhesion and Ag diffusion barrier properties for Ag/PPy composites. To broadly use Ag/PPy composites as a TSV filling material in the future, it is crucial to understand the interface reactions between the composite and the Si. Currently, while many articles are focusing on the structural or electrical properties of the Ag/PPy material, no thorough research has been made about its reactions with other materials/substrates. To improve throughput for production of 3D-LSI by reducing the process steps, the role of SiO_x and SiN_x as a diffusion barrier layer for Ag and C is examined.

2. EXPERIMENTAL PROCEDURES

2.1. Materials and Synthesis. The Ag/PPy composite was initially prepared into dispersion before applying on the Si substrates (sample size: 5 × 5 mm^2). PPy was synthesized by silver nitrate ($AgNO_3$) (1.0 mol·dm^{-3}) as dopant and metal salts for oxidant and pyrrole monomer (0.2 mol·dm^{-3}) used for polymerization in acetonitrile (CH_3CN) solvent (2.5 cm^{-3}). The reaction was photoassisted by UV irradiation (with an intensity of 50 mW·cm^{-2} for 10 min), increasing the growth rate of the composite. Four types of substrates were examined: Si(100) with its native oxide or coated with Si oxide (SiO_x) or Si-oxynitride (SiON-1 and SiON-2) barrier layers. For the samples provided with Si oxide barrier layers, SiO_x was deposited on the substrate by thermal oxidation (parameters: dry oxidation at 1050 °C for 3h 10 min) to an initial 200 nm thickness and was etched to the desired thicknesses by hydrofluoric acid (HF) (parameters: HF/NH_4F = 1:6; etching time: 0, 30, 60, 90 s). The developed SiO_x thicknesses were 10, 50, and 100 nm. The substrates with Si-oxynitride barrier layers were deposited by physical vapor deposition technique (apparatus: Shibaura Mechatronics Corporation, i-Miller CFS-4EP-LL) onto SiON-1 (parameters: Ar 28 sccm, N_2 10 sccm, DC 330 W, 0.511 Pa) and SiON-2 (parameters: Ar 18 sccm, N_2 10 sccm, DC 330 W, 0.379 Pa). Similarly to the case of SiO_x, the created SiON layer thicknesses were 10, 50, and 100 nm. The substrate was then immersed into the dispersion. After removal of the sample from the dispersion, it was dried in ambient conditions.

2.2. Characterization. Initially, X-ray photoelectron spectroscopy (XPS; Thermo Electron Co., Theta Probe, 3 kV) was used to verify the composition of the barrier layers, and the thickness was confirmed by ellipsometry (J.A. Woollam M-2000). The composite itself and the layer structures were investigated for structural and interfacial analysis after the deposition by 150 h in room temperature. Adhesiveness of the composite on the substrate was evaluated by the peel-off test in accordance with the Japan Industrial Standard (JIS) Z 1522 on six samples per barrier layer type. Twenty-four hours after the deposition of the coating, cellophane tape (15 mm in width, Nichiban LP-15) was stuck to the whole surface of the specimen and detached vertically within 0.5 s. The morphology of the developed composite was observed by scanning electron microscopy (SEM) (Hitachi S-4800, 20 kV). The samples were etched with focused ion beam (FIB; JEOL JEM-9320FIB, 30 kV), and the microstructures and chemical compositions were observed by transmission electron microscopy (TEM; JEOL 2100-F, 200 kV and FEI Technai G2 F30, 300 kV) equipped with energy-dispersive X-ray spectroscopy (EDX), electron energy loss spectroscopy (EELS), and selected area electron diffraction (SAED). Before measuring the C element with EELS, the samples were treated with ion cleaning.

3. RESULTS AND DISCUSSION

3.1. Structure of Ag/PPy Composite on Si. When applying Ag/PPy composite coating on a Si surface, the composite material is composed of PPy material, and the Ag segregates into clusters within. The size of the Ag clusters can vary between from a few nanometers to up to tens of micrometers, and they are located in the PPy in very high density. Nanosized particles are situated very close to each other between two large Ag clusters, conferring good conductivity to the material. High-resolution (HR) TEM images show the Ag particles in dark gray and the surrounding PPy in light gray (Figures 1 and 2). EDX analysis on the area

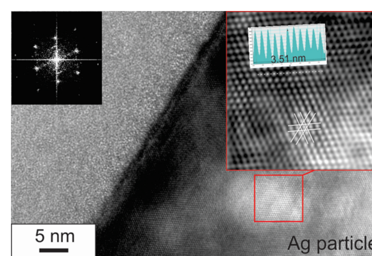

Figure 1. HRTEM image of the Ag nanoparticle with the FFT and filtered inversed FFT image of the area in red rectangle.

surrounding Ag (C, 72.26; N, 17.50; O, 5.46; Si, 2.26; Ag, 2.52 atom %) confirms the mass presence of C and N with a suitable ratio for PPy composition. It can be seen that the structure of the PPy is amorphous. To properly identify the atomic structure, Fast Fourier transform (FFT), a filter, and then inversed FFT were used. HRTEM images confirmed the fcc crystalline structure of bulk Ag (Figure 1), and the structure of the Ag nanoparticles can be single-crystalline (Figure 2a) or polycrystalline (Figure 2b), often (but not mainly) depending on the size of the particle. On the single crystalline nanoparticle, the spacing of atoms is measured to be 0.35

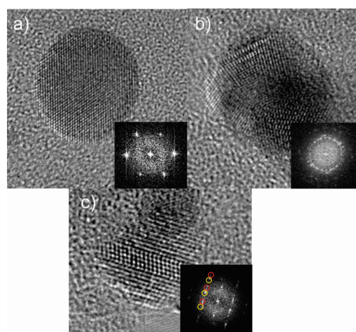

Figure 2. HRTEM image of the Ag cluster with the corresponding diffraction pattern: (a) single crystalline, (b) polycrystalline, and (c) twin structure.

nm, which correlates to the lattice constant of the fcc cubic crystal structure Ag(111) plane. The lattice constant of Ag is a = 4.085 Å, and the spacing of the (111) plane is

$$b = d/2 = (a\sqrt{3})/2 = 3.537 \text{ Å} \quad (1)$$

The diffraction patterns measured on the entire Ag particle shows the diffraction pattern of the (111) plane.

In some cases, a twin structure is visible in the Ag nanoparticle (Figure 2c). Twinning occurs within the nanoparticle when a crystal shares lattice points on the face of another crystal, but grows with a different orientation due to an interruption (such as mis-stacking of atoms). Here, the diffraction pattern verifies the twinning with the yellow diffraction showing the base and the corresponding red diffraction dot representing the twin. Twinning can be responsible for polycrystalline Ag particles, as the growth-mediated formation may proceed by cyclic twinning operations due to misstacking of atoms during growth.[36]

Figure 3a shows a cross-sectional HRTEM image of the Ag/PPy composite and Si interface. EDX analysis of the layer

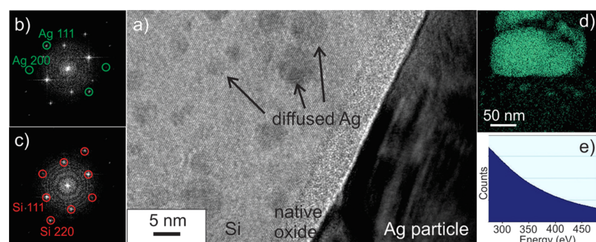

Figure 3. (a) HRTEM image of the Si/composite interface (native oxide in between), with signs of diffused Ag, with corresponding diffraction of the area (b) with and (c) without the diffused Ag. (d) Ag element map of the interfacial structure of the Ag/PPy composite and Si substrate. (e) EELS spectrum of the Si substrate area.

structure shows considerable amounts of Ag diffused in segregated particles underneath the Si substrate near the interface. Ag particles were found in the substrate in up to 1−2 μm depth. These Ag atoms originated from the Ag clusters in the Ag/PPy composite. Ag is a fast diffuser in Si oxide even at lower temperatures,[34] which explains how the Ag penetrated through the protecting thin Si oxide layer. The Ag particles showed up to 22 atom % Ag atom content in these certain clusters, and the FFT of the particles shows the structure is crystalline Ag, meaning that the Ag_2Si silicide phase did not form in this case. The regions with diffused Ag are indicated with arrows. Diffraction patterns show that in areas where Ag is not present, the Si substrate has a single crystal structure, while in areas with Ag diffusion present crystalline Ag diffraction patterns can be found within the layer (Figure 3b, c). Also, confirming the EDS results, diffraction spots of Ag_2Si are not visible. Normally, Ag atoms are most frequently incorporated interstitially within dislocation-free Si.[28] The segregating Ag (as visible in Figure 3d) suggests existing dislocations within the Si substrate. The dislocations interact with impurities, causing higher concentrations of Ag to segregate in Si with dislocations than in dislocation-free areas, and Ag is transformed from interstitial to substitutional Ag by the theory of interstitial-substitutional diffusion mechanisms.

Diffusion of C within the Si substrate has not been observed on any of the samples, neither on Si with native oxide nor on Si equipped with SiO_x, SiON barriers. While occasionally small quantities of C were detected with EDX or FFT, the source of this C is only contamination. Ion cleaning has damaging properties on the Ag/PPy layer; therefore, it had to be conducted after the major TEM measurements. EELS measurements conducted directly after ion cleaning proves that no C exists in the Si or the barriers, as EELS spectra show no C peak at 284 eV (Figure 3e).

The Si oxide between the Si substrate and the Ag/PPy composite shows unusual properties. When Si surfaces are exposed to air under ambient circumstances, native oxide (SiO_2) normally has a thickness of 1 nm.[37] In this case, the samples were analyzed with ellipsometry prior to coating and had a uniform 0.98 nm oxide layer. After coating, TEM measurements show the oxide layer thickness to grow to 5.8 nm. Figure 4 shows the HRTEM image of the oxide layer

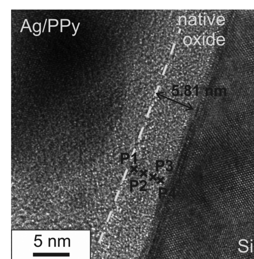

Figure 4. Cross-sectional HRTEM image of the developed oxide layer with the corresponding EDX values (P1−P4) in Table 1.

which shows amorphous structure in the layer. EDX measurements (Table 1) show that the composition of this new layer is

Table 1. Composition of the New Oxide Layer Developed on Si by the Ag/Py Composite [atom %]

	C	N	O	Si	Ag
P1	0.00	0.00	34.36	65.42	0.22
P2	0.00	0.00	28.83	70.29	0.88
P3	0.00	0.00	20.98	78.88	0.14
P4	0.00	0.00	18.51	80.87	0.63

a mixture of 65−80% Si and 18−35% O with less than 1% Ag corresponding to the Ag particles passing through the layer toward the Si substrate. The unusual oxide thickness may be caused by the oxidation of Si with NO_3^- ions located in the composite dispersion when placing on the surface.

3.2. Diffusion Properties of Ag/PPy on Different Barriers. Interface examination between Si-oxide barrier layers

dx.doi.org/10.1021/am501305b | ACS Appl. Mater. Interfaces 2014, 6, 9201−9206

and Ag/PPy shows the following results. Application of a 10 nm layer demonstrated little improvement for preventing the diffusion; elemental maps show Ag to break through the SiO_x barrier. The Ag particles diffused up to 600 nm into the substrate (Figure 5a, b). Diffraction patterns measured on the substrate in Figure 5c show pure Si in the light areas and diffused Ag as dark spots.

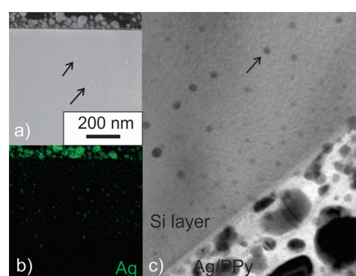

Figure 5. Interface examinations on a 10 nm thick SiO_x barrier layer. (a) DF TEM image with the arrows showing the Ag particles. (b) Ag element map of the Si layer. (c) HRTEM image of the Si layer near or further from the Ag region.

The application of 50 and 100 nm thick oxide layers demonstrated slightly improved results. In these cases, Ag diffusion was observed to around 100 and 50 nm deep within the Si layer, respectively (Figure 6a) with only a few additional

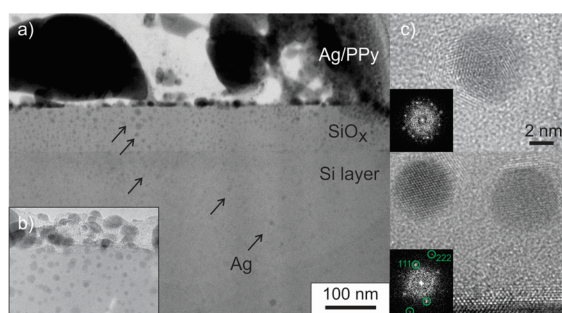

Figure 6. Interface examinations on a 100 nm thick SiO_x barrier layer. (a) BF TEM image with arrows showing the Ag particles. HRTEM image of (b) the composite/oxide interface and (c) the polycrystalline and single crystalline Ag particles inside the oxide layer (with FFT).

particles diffusing under this depth limit. In these cases, the Ag content of the identified particles (dark spots) within the Si is low (<5 atom %), while in the light areas the Ag content is zero. Within the oxide layer, examinations on the Ag particles show crystalline structure of the Ag. Here, the size of the particles is strongly decreased, and all particles measured between 2 and 6 nm (Figure 6b). FFT diffraction analysis of the Ag particles inside the oxide layer in the HRTEM image (Figure 6c) shows a single-crystalline FCC structure in most of the cases; however, some particles were found to be polycrystalline. The transport of the Ag particles occurs by the particles entering into the oxide through the weakened areas in the lattice by broken Si−O−Si bridges.[38,39] If the original Ag cluster inside the composite material is a larger mono- or polycrystalline structure, the Ag particle entering the oxide layer will most probably a small section of the grain (or for polycrystalline, originated from the nearest grain to the composite/oxide interface) entering into the oxide layer and becomes an independent single crystalline particle. The particles only stay polycrystalline inside the oxide if the original Ag particle in the composite was also in the same 2−6 nm size range and the entire particle could slip through the composite/oxide interface without structural modification. This hypothesis is supported by the ratio of single crystals/polycrystals in both layers; while in the composite the nanosized particles are mostly polycrystalline and the larger particles are mostly single crystals or equipped with only few crystal orientations, in the oxide layer the large majority of the nanoparticles are single crystals.

Diffusion resisting effects of the Si-oxynitrate barrier layers were also examined, and both SiON-1 and SiON-2 (referred together as SiON) showed similar good barrier properties to Ag, as is well-known for SiN_x. Ag diffusion was blocked with SiON layers as thin as 10 nm, as EDX and diffraction measurements show no trace in the Si and the Si-oxynitride layer (Figure 7).

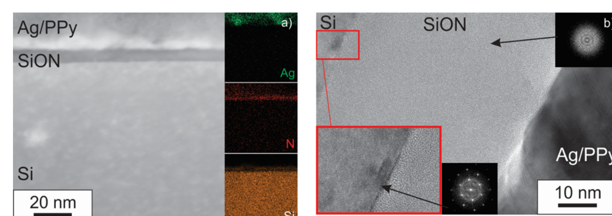

Figure 7. Interface examinations of SiON-2 barrier layer. (a) TEM image of a 10 nm layer with EDX mapping. (b) HRTEM image with FFT of the Si and the 100 nm thick layer.

3.3. Adhesion Properties of Ag/PPy on Different Barriers.

In the current research, a peel-off test was used to evaluate the adhesion of Ag/PPy with the three types of substrates. Figure 8a shows the resulting specimen surface after

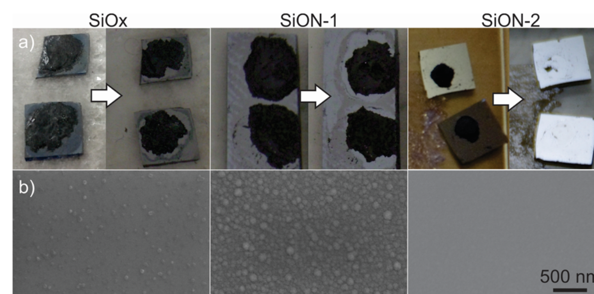

Figure 8. Comparison between SiO_x, SiON-1, and SiON-2 layers. (a) Peel-off strength test. (b) Morphology of the layers.

the peel-off test. While for SiON-1 and SiO_x the composite remained on the surface in acceptable amounts (>90%), SiON-2 failed the test and the composite peeled off with the adhesive cellophane tape. The morphology of the layers, observed by SEM, shows that while SiO_x has a slightly and SiON-1 has a heavily rough surface with bumps of approximately 40 and 60 nm, respectively, SiON-2 has a very smooth surface (Figure 8b). The morphology of the surface oxide on the metal plays strong role in the strength of metal−polymer bonds where porosity and microscopic roughness mechanically interlock with the polymer, forming much stronger bonds than on smooth surfaces.[40,41] Measurements with XPS verify the composition of the layers to be amorphous silicon nitride of the following composition: SiON-1, $Si_{55}N_{40}O_5$; SiON-2,

$Si_{53}N_{45}O_2$; SiO_x, Si_2O_3. At the polymer/metal interface, chemical bonding occurs between the metal substrates and the polymer[42] and their adherence depends on the formation of primary and secondary bonds within the interface. Oxygen on metal surfaces has a strong influence on bond line strength: moisture absorption leads to the formation of hydroxyl groups which can react with polar groups in the adhesive.[43] The higher oxygen content and rough surface of the SiON-1 and SiO_x barrier layers explain the good adhesion properties of Ag/PPy on these surfaces. Additionally, for SiO_x, the Ag diffusion into the barrier layer and substrate also helps the composite adhesion (although it is an unwanted phenomenon for reliability issues). The smooth surface and low oxygen content of SiON-2 is responsible for the poor adhesion toward the Ag/PPy composite.

According to our research, SiON-1 barrier layers of as little as 10 nm are a perfect solution for TSV when using Ag/PPy composites as a via filling material. The high N content is a perfect Ag barrier layer, while the moderate O content and high surface roughness is suitable for the good adhesion of the Ag/PPy material.

4. CONCLUSION

With the use of barrier layers, the Ag/PPy composites described herein are a good candidate for the conductive filling of TSV in 3D-LSI devices using a fast and inexpensive fabrication process to create vertical electrical wiring for advanced 3D semiconductor devices. Clarification of the interfacial structure has been made, and an optimized barrier layer has been established with good adhesion and diffusion barrier properties. The examinations show the following results:

After deposition of the composite on Si substrate (with native oxide layer), Ag diffusion occurs toward the Si layer originating from the Ag clusters in the Ag/PPy composite. Ag segregation is observed around the dislocations within the Si substrate. Ag/PPy forms 5 times larger Si oxide on the Si substrate than the thickness of the developed native oxide under ambient conditions.

Diffusion of C within the Si substrate has not been observed on any of the samples, neither on Si with native oxide nor on Si coated with SiO_x, SiON barriers.

Ag from the composite can migrate through even 100 nm thick SiO_x, although the amount of Ag diffused into Si decreases with increasing thickness of the barrier layer. The N content of SiON-1 and SiON-2 completely blocks the diffusion of Ag toward Si through thicknesses as little as 10 nm. While SiON-2 has poor adhesion due to the inadequate amount of O in its layer and smooth surface, the 5% O content and rough surface of SiON-1 make it a suitable solution for TSV barrier material.

The Ag clusters within the PPy have a single-crystalline or polycrystalline structure resulting from cyclic twinning, and the size can vary between from a few nanometers to up to tens of micrometers. However, during the diffusion of Ag through the Si oxide layer, the Ag particles break down into 2−6 nm size and in most of the cases single-crystalline structure.

AUTHOR INFORMATION

Corresponding Author

*E-mail: bhorvath@ett.bme.hu.

Author Contributions

The manuscript was written with contributions of all authors. All authors have given approval to the final version of the manuscript.

Notes

The authors declare no competing financial interest.

ACKNOWLEDGMENTS

This research was financially supported by Adaptable & Seamless Technology Transfer Program through Target-driven R&D (A-STEP) of Japan Science and Technology Agency and by Grants-in-Aid for Scientific Research (KAKENHI) of Japan Society for the Promotion of Science. The silicon wafer with vertical holes was supplied by Research Center for Three-Dimensional Semiconductors, Fukuoka Japan. The SiOx and SiON layers were done in the MANA Foundry, NIMS.

REFERENCES

(1) Motoyoshi, M. Through-Silicon Via (TSV). *Proc. IEEE* **2009**, *97*, 43−48.

(2) Okoro, C.; Vanstreels, K.; Labie, R.; Lühn, O.; Vandevelde, B.; Verlinden, B.; Vandepitte, D. Influence of Annealing Conditions on the Mechanical and Microstructural Behavior of Electroplated Cu-TSV. *J. Micromech. Microeng* **2010**, *20*, 045032.

(3) Kim, B.; Sharbono, C.; Ritzdorf, T.; Schmauch, D. Factors Affecting Copper Filling Process Within High Aspect Ratio Deep Vias for 3D Chip Stacking. *Proc. − Electron. Compon. Technol. Conf. 56th* **2006**, 838−843.

(4) Shi, S.; Wang, X.; Xu, C.; Yuan, J.; Fang, J.; Liu, S. Simulation and Fabrication of Two Cu TSV Electroplating Methods for Wafer-Level 3D Integrated Circuits Packaging. *Sens. Actuators, A* **2013**, *203*, 52−61.

(5) Okoro, C.; Labie, R.; Vanstreels, K.; Franquet, A.; Gonzalez, M.; Vandevelde, B.; Beyne, E.; Vandepitte, D.; Verlinden, B. Impact of the Electrodeposition Chemistry Used for TSV Filling on the Microstructural and Thermo-Mechanical Response of Cu. *J. Mater. Sci.* **2011**, *46*, 3868−3882.

(6) Arunagiri, T. N.; Zhang, Y.; Chyan, O.; El-Bouanani, M.; Kim, M. J.; Chen, K. H.; Wu, C. T.; Chen, L. C. 5nm Ruthenium Thin Film as a Directly Plateable Copper Diffusion Barrier. *Appl. Phys. Lett.* **2005**, *86*, 083104.

(7) Stejskal, J. Conducting Polymer-Silver Composites. *Chem. Pap.* **2013**, *67*, 814−848.

(8) Fujii, S.; Matsuzawa, S.; Hamasaki, H.; Nakamura, Y.; Bouleghlimat, A.; Buurma, N. J. Polypyrrole−Palladium Nanocomposite Coating of Micrometer-Sized Polymer Particles Toward a Recyclable Catalyst. *Langmuir* **2011**, *28*, 2436−2447.

(9) Tamil Selvan, S. Novel Nanostructures of Gold-Polypyrrole Composites. *Chem. Commun.* **1998**, *3*, 351−352.

(10) Henry, M. C.; Hsueh, C.-C.; Timko, B. P.; Freund, M. S. Reaction of Pyrrole and Chlorauric Acid A New Route to Composite Colloids. *J. Electrochem. Soc.* **2001**, *148*, D155−D162.

(11) Kawakita, J.; Chikyow, T. Fast Formation of Conductive Material by Simultaneous Chemical Process for Infilling Through-Silicon Via. *Jpn. J. Appl. Phys.* **2012**, *51*, 06FG11.

(12) Jung, Y. J.; Govindaiah, P.; Choi, S. W.; Cheong, I. W.; Kim, J. H. Morphology and Conducting Property of Ag/Poly(pyrrole) Composite Nanoparticles: Effect of Polymeric Stabilizers. *Synth. Met.* **2011**, *161*, 1991−1995.

(13) Shi, Z.; Wang, H.; Dai, T.; Lu, Y. Room Temperature Synthesis of Ag/Polypyrrole Core−shell Nanoparticles and Hollow Composite Capsules. *Synth. Met.* **2010**, *160*, 2121−2127.

(14) Dallas, P.; Niarchos, D.; Vrbanic, D.; Boukos, N.; Pejovnik, S.; Trapalis, C.; Petridis, D. Interfacial Polymerization of Pyrrole and In Situ Synthesis of Polypyrrole/Silver Nanocomposites. *Polymer* **2007**, *48*, 2007−2013.

(15) Zhao, C.; Zhao, Q.; Zhao, Q.; Qiu, J.; Zhu, C.; Guo, S. Preparation and Optical Properties of Ag/PPy Composite Colloids. *J. Photochem. Photobiol., A* **2007**, *187*, 146−151.
(16) Ijeri, V. S.; Nair, J. R.; Gerbaldi, C.; Gonnelli, R. S.; Bodoardo, S.; Bongiovanni, R. M. An Elegant and Facile Single-Step UV-Curing Approach to Surface Nano-Silvering of Polymer Composites. *Soft Matter* **2010**, *6*, 4666−4668.
(17) Kabir, L.; Mandal, A. R.; Mandal, S. K. Humidity-Sensing Properties of Conducting Polypyrrole-Silver Nanocomposites. *J. Exp. Nanosci.* **2008**, *3*, 297−305.
(18) Kate, K. H.; Damkale, S. R.; Khanna, P. K.; Jain, G. H. Nano-Silver Mediated Polymerization of Pyrrole: Synthesis and Gas Sensing Properties of Polypyrrole (PPy)/Ag Nano-Composite. *J. Nanosci. Nanotechnol.* **2011**, *11*, 7863−7869.
(19) Qin, X.; Lu, W.; Luo, Y.; Chang, G.; Sun, X. Preparation of Ag Nanoparticle-Decorated Polypyrrole Colloids and their Application for H2O2 Detection. *Electrochem. Commun.* **2011**, *13*, 785−787.
(20) Yao, T.; Wang, C.; Wu, J.; Lin, Q.; Lv, H.; Zhang, K.; Yu, K.; Yang, B. Preparation of Raspberry-like Polypyrrole Composites with Applications in Catalysis. *J. Colloid Interface Sci.* **2009**, *338*, 573−577.
(21) Shi, Z.; Zhou, H.; Qing, X.; Dai, T.; Lu, Y. Facile Fabrication and Characterization of Poly(tetrafluoroethylene)@Polypyrrole/Nano-Silver Composite Membranes with Conducting and Antibacterial Property. *Appl. Surf. Sci.* **2012**, *258*, 6359−6365.
(22) Firoz Babu, K.; Dhandapani, P.; Maruthamuthu, S.; Anbu Kulandainathan, M. One Pot Synthesis of Polypyrrole Silver Nanocomposite on Cotton Fabrics for Multifunctional Property. *Carbohydr. Polym.* **2012**, *90*, 1557−1563.
(23) Horváth, B.; Kawakita, J.; Chikyow, T. Through Silicon Via Filling Methods with Metal/Polymer Composite for Three-Dimensional LSI. *Jpn. J. Appl. Phys.* **2014**, *53*, 06JH01.
(24) Kawakita, J.; Hashimoto, Y.; Chikyow, T. Strong Adhesion of Silver/Polypyrrole Composite onto Plastic Substrates toward Flexible Electronics. *Jpn. J. Appl. Phys.* **2013**, *52*, 06GG12.
(25) Seino, K.; Schmidt, W. G.; Furthmüller, J.; Bechstedt, F. Chemisorption of Pyrrole and Polypyrrole on Si(001). *Phys. Rev. B* **2002**, *66*, 235323.
(26) Coffa, S.; Poate, J. M.; Jacobson, D. C.; Frank, W.; Gustin, W. Determination of Diffusion Mechanisms in Amorphous Silicon. *Phys. Rev. B* **1992**, *45*, 8355−8358.
(27) Kawamoto, K.; Mori, T.; Kujime, S.; Oura, K. Observation of the Diffusion of Ag Atoms Through an a-Si layer on Si(111) byLow-Energy Ion Scattering. *Surf. Sci.* **1996**, *363*, 156−160.
(28) Rollert, F.; Stolwijk, N. A.; Mehrer, H. Solubility, Diffusion and Thermodynamic Properties of Silver in Silicon. *J. Phys. D: Appl. Phys.* **1987**, *20*, 1148.
(29) Klumpp, A.; Ramm, P.; Wieland, R. In *3D-Integration of Silicon Devices: A Key Technology for Sophisticated Products*, Proceedings of the Design, Automation & Test in Europe Conference & Exhibition, 8−12 March 2010; pp 1678−1683.
(30) Sage, S.; John, P.; Dobritz, S.; Börnge, J.; Vitiello, J.; Böttcher, M. Investigation of Different Methods for Isolation in Through Silicon Via for 3D Integration. *Microelectron. Eng.* **2013**, *107*, 61−64.
(31) Hoornstra, J.; Schubert, G.; Broek, K.; Granek, F.; LePrince, C. In *Lead Free Metallisation Paste for Crystalline Silicon Solar Cells: from Model to Results*, Proceedings of the Photovoltaic Specialists Conference, IEEE, 3−7 Jan 2005; pp 1293−1296.
(32) Acton, Q. A. *Heavy Metals—Advances in Research and Application*, 2013 ed.; ScholarlyEditions: Atlanta, GA, 2013.
(33) Suryanarayana, D.; Mittal, K. L. Effect of Polyimide Thickness on its Adhesion to Silicon Nitride Substrate with and without Adhesion Promoter. *J. Appl. Polym. Sci.* **1985**, *30*, 3107−3111.
(34) McBrayer, J. D.; Swanson, R. M.; Sigmon, T. W. Diffusion of Metals in Silicon Dioxide. *J. Electrochem. Soc.* **1986**, *133*, 1242−1246.
(35) Kim, H.-K.; Cho, C.-K. Transparent SiON/Ag/SiON Multilayer Passivation Grown on a Flexible Polyethersulfone Substrate Using a Continuous Roll-to-Roll Sputtering System. *Nanoscale Res. Lett.* **2012**, *7* (69), 1−6.
(36) Hofmeister, H. Fivefold Twinned Nanoparticles. *Encycl. Nanosci. Nanotechnol.* **2003**, *3*, 431−452.
(37) Morita, M.; Ohmi, T.; Hasegawa, E.; Kawakami, M.; Ohwada, M. Growth of Native Oxide on a Silicon Surface. *J. Appl. Phys.* **1990**, *68*, 1272−1281.
(38) Revesz, A. G.; Evans, R. J. Kinetics and Mechanism of Thermal Oxidation of Silicon with Special Emphasis on Impurity Effects. *J. Phys. Chem. Solids* **1969**, *30*, 551−564.
(39) Dallaporta, H.; Liehr, M.; Lewis, J. E. Silicon Dioxide Defects Induced by Metal Impurities. *Phys. Rev. B* **1990**, *41*, 5075−5083.
(40) Venables, J. D. Adhesion and Durability of Metal-Polymer Bonds. *J. Mater. Sci.* **1984**, *19*, 2431−2453.
(41) Bijlmer, P. F. A. Influence of Chemical Pretreatments on Surface Morphology and Bondability of Aluminium. *J. Adhes.* **1973**, *5*, 319−331.
(42) Ramarathnam, G.; Libertucci, M.; Sadowski, M. M.; North, T. H. Joining of Polymers to Metal. *Weld. J.* **1992**, *71*, 483-s−490-s.
(43) Kozma, L.; Olefjord, I. Surface Treatment of Steel for Structural Adhesive Bonding. *Mater. Sci. Technol.* **1987**, *3*, 954−962.